

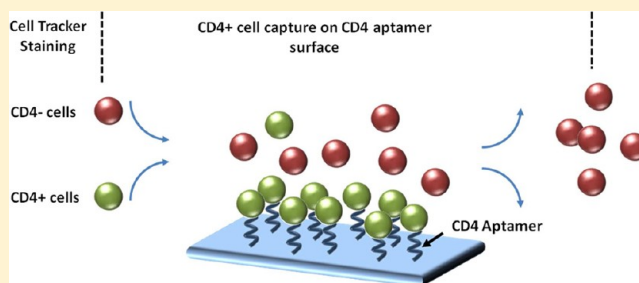
Aptamer-Containing Surfaces for Selective Capture of CD4 Expressing Cells

Qing Zhou, Ying Liu, Dong-Sik Shin, Jaime Silangcruz, Nazgul Tuleuova, and Alexander Revzin*

Department of Biomedical Engineering, University of California, Davis, California 95616, United States

Supporting Information

ABSTRACT: Aptamers have recently emerged as an excellent alternative to antibodies because of their inherent stability and ease of modification. In this paper, we describe the development of an aptamer-based surface for capture of cells expressing CD4 antigen. The glass or silicon surfaces were modified with thiolated RNA aptamer against CD4. Modification of the surface was first characterized by ellipsometry to demonstrate assembly of biointerface components and to show specific capture of recombinant CD4 protein. Subsequently, surfaces were challenged with model lymphocytes (cell lines) that were either positive or negative for CD4 antigen. Our experiments show that aptamer-functionalized surfaces have similar capture efficiency to substrates containing anti-CD4 antibody. To mimic capture of specific T-cells from a complex cell mixture, aptamer-modified surfaces were exposed to binary mixtures containing Molt-3 cells (CD4+) spiked into Daudi B cells (CD4-). 94% purity of CD4 cells was observed on aptamer-containing surfaces from an initial fraction of 15% of CD4. Given the importance of CD4 cell enumeration in HIV/AIDS diagnosis and monitoring, aptamer-based devices may offer an opportunity for novel cell detection strategies and may yield more robust and less expensive blood analysis devices in the future.



INTRODUCTION

Leukocytes (white blood cells) play a major role in the immune response against pathogenic infections. T-helper cells (CD4+ T-cells) are one of the most important immune cells. They are responsible for regulating immune cell recruitment and proliferation through cell–cell interactions and cytokine production.¹ Aberrations in the amount and types of cytokines produced by CD4+ T-cells can lead to immunodeficiency, autoimmunity, and allergies.^{2–5} Furthermore, the loss of CD4+ T-cells following HIV infection leads to AIDS;^{6–8} therefore, analysis of CD4+ T-cells remains an active area of study, in both clinical diagnostics and basic immunology research.⁹

The bioengineering community has been active in developing devices for leukocyte capture and analysis.^{10–19} These studies have focused on integrating surfaces modified with monoclonal antibodies into microfluidic devices in order to minimize the sample volume and to enable panning of specific cell subsets such as CD4 cells. While these efforts have yielded devices suitable for CD4 detection in clinical setting,^{18,20} the reliance on antibodies for cell capture may be suboptimal from the standpoint of limited thermal/chemical stability of these molecules. In addition, detecting CD4 cells either requires optical detection^{19,20} or necessitates development of sophisticated electrical detection strategies.^{20,21}

We sought to investigate the use of aptamers for capture of CD4 expressing cells. Aptamers are single-stranded oligonucleotides (RNA or DNA) that are able to recognize and bind targets with specificity comparable to antibodies because of

their ability to fold into distinct secondary and tertiary structures.²² Because of their oligonucleotide structure, aptamers offer a number of advantages over antibodies including an inexpensive, rapid, and reproducible synthesis pathway; easily implemented chemical modification approaches; long-term stability; and the potential reusability. Importantly, aptamers have been modified with fluorescence or electrochemical reporter molecules to enable reagentless detection of analyte.^{23–26} Thus, aptamers are particularly suited for development of biosensors requiring limited handling or washing steps which makes them particularly promising for point of care applications. The use of aptamers have previously been demonstrated for the capture and enrichment of several cell types including mesenchymal stem cells, osteoblasts, lymphoblasts, and circulating tumor cells.^{27–33} However, despite the fact that a sequence of anti-CD4 aptamer has been reported in the literature³⁴ and used for fluorescent labeling of CD4 T-cells, to the best of our knowledge aptamer-functionalized surfaces have not been used for the capture of CD4+ T-cells.

In this report, we describe the use of aptamer-modified surfaces for capturing model CD4+ T-cells. To this end, anti-CD4 aptamer as well as nonsense aptamer were immobilized on aminosilane-modified glass or silicon substrates via

Received: December 20, 2011

Revised: July 29, 2012

Published: August 1, 2012

maleimide--NHS heterobifunctional linker (see Figure 1). The surfaces were incubated with recombinant CD4 and CD8

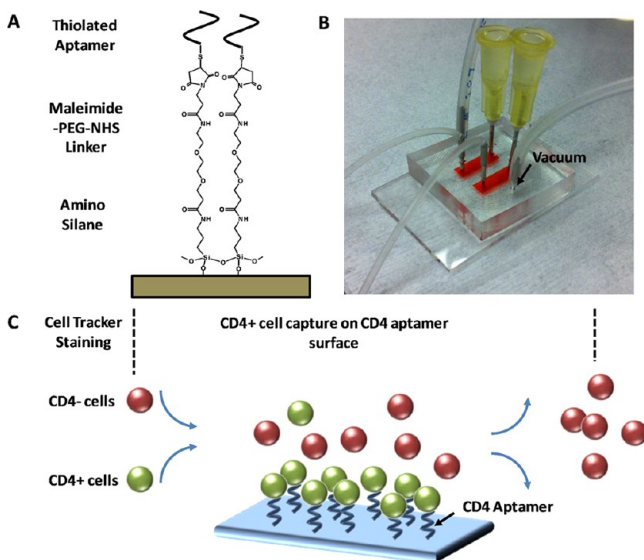


Figure 1. (A) Diagram of aptamer binding scheme on the glass surface. (B) Photo of the two channel device containing the aptamer-functionalized surface and PDMS on top; the PDMS was reversibly secured onto the substrate via the negative pressure produced by vacuum applied in the auxiliary network around the two chambers. Food dye was used to highlight the two fluid chambers. (C) Scheme illustrating selective capture of CD4+ cells on CD4 aptamer-immobilized surface. The colors of the cells represent CD4+ and CD4- cells stained with different cell tracker dyes.

proteins and characterized by ellipsometry to demonstrate that CD4 antigen bound to the specific aptamer. In subsequent experiments, aptamer-modified surfaces were integrated into microfluidic devices and infused with mixtures of model CD4 (+) and CD4 (-) cells, demonstrating capture of CD4 expressing cells on CD4 aptamer surfaces (Figure 1B,C). Significantly, incubation of aptamer-functionalized surfaces with a binary mixture of specific and nonspecific cells resulted in 6-fold enhancement in density of CD4 expressing cell on substrate, from 15% in solution to 94% on the surface. Overall, our results demonstrate that surfaces modified with RNA aptamer specific to CD4 antigen may be used to capture and enrich CD4 expressing cells. In the future, aptamers may be further modified to introduce reporter moieties to enable detection of cell binding events. These surfaces may also be combined with aptamer beacons for cytokine detection^{35–37} in order to develop antibody-free, all-aptamer devices for capture and analysis of specific cell populations.

MATERIALS AND METHODS

Materials. 1x phosphate-buffered saline without calcium and magnesium (PBS), anhydrous toluene (99.8%), bovine serum albumin (BSA), ethylenediaminetetraacetic acid (EDTA), potassium bicarbonate (KHCO₃), ammonium chloride (NH₄Cl), magnesium chloride (MgCl₂), 2-hydroxy-2-methylpropiophenone (HMPP), (3-acryloxypropyl)trimethoxysilane (acrylsilane), and 3-aminopropyltrimethoxysilane (aminosilane) were purchased from Gelest, Inc. (Morrisville, PA). Glass slides (75 × 25 mm²), coverslips, and cell culture medium RPMI 1640 with L-glutamine were purchased from VWR. Medium was supplemented with fetal bovine serum (FBS), and penicillin/streptomycin purchased from Invitrogen (Carlsbad, CA). MAL-dPEG₂-NHS ester (linker) was purchased from Quanta

Biodesign, Ltd. (Powell, OH). Formalin solution was purchased from Fisher Scientific (Waltham, MA). Antihuman CD4 (13B8.2) was purchased from Beckman-Coulter (Brea, CA). Antihuman CD4 antibody was purchased from BD Biosciences (San Diego, CA). Recombinant CD4 and CD8 antigen were purchased from Creative Biomart (Shirley, NY). CellTracker Green CMFDA (5-chloromethylfluorescein diacetate) and CellTracker Red CMTPX were purchased from Invitrogen (Eugene, OR). Human acute lymphoblastic T-cells (MOLT-3) were purchased from American Type Culture Collection (Manassas, VA). Sylgard 184 poly(dimethylsiloxane) (PDMS) along with a curing agent were purchased from Dow Corning (Midland, MI). Deionized water (diH₂O) was used from an in-building system providing water with resistivity greater than 17.5 MΩ cm². Thiolated antihuman CD4 aptamer was synthesized and purified by Integrated DNA Technologies (Coralville, IA). The sequence and modification of the CD4 aptamer are as follows:

5'-thiol-C6-GUGACGUCUGAUCGAUUGUGCAUUCGGU-GUGACGAUCU-3'³⁴

A nonsense aptamer for IFN-γ was used as a control in our experiments. Its sequence is as follows:

5'-thiol-C6-GGGGTTGGTTGTGTTGGGTTGTTGTGTC-AACCC-3'

Aptamers purified after RNase free high-performance liquid chromatography were stored in nuclease-free water at -20 °C until use. 1x PBS containing 2 mM MgCl₂ was added to the buffer used for protein and cell binding experiments. Prior to use, aqueous aptamer solution added to buffer to achieve the needed concentration and heated to 80 °C for 3 min, chilled on ice, and then transferred to room temperature prior to commencing experiments.

Immobilization of Aptamers. Glass surfaces were functionalized using standard silanization protocols. Briefly, glass slides were exposed to O₂ plasma for 5 min at 300 W, placed into a N₂-filled glovebag, and immersed in 0.1% v/v (3-acryloxypropyl)trimethoxysilane and 3-aminopropyltrimethoxysilane mix in anhydrous toluene. The silane self-assembly reaction was allowed to proceed for 5 h under N₂, after which slides were rinsed in fresh toluene, dried under nitrogen, and placed in an oven for 2 h at 100 °C to ensure cross-linking of the silane layer. Samples were stored in a desiccator prior to use. Immediately before aptamer immobilization, silanized substrates were immersed in 10 mM maleimide-NHS linker for 1 h to create thiol-reactive glass substrates. These surfaces were rinsed with 1x PBS and diH₂O and dried under N₂.

Ellipsometric Measurements of Surfaces. Construction of the biointerface consisting of silane, linker, and aptamer (see Figure 1A for chemical structure) was characterized using an LSE Stokes ellipsometer (Gaertner Scientific). In these experiments, 4 in. silicon wafers (University Wafers) were diced into smaller pieces (0.5 × 0.5 in.) and functionalized with silane, linker, and aptamer using exactly the same protocol described above for glass surfaces. The substrates were modified with aptamers against CD4 as well as nonsensing aptamers against IFN-γ described by us previously.^{35,36} After functionalization, the substrates were incubated with 10 μM CD4 protein or with nonsense CD8 protein. Ellipsometric measurements were taken after assembly of each layer. Thickness of each layer was calculated using an optical model assuming uniform, isotropic, parallel slabs. Optical constants were obtained from the silicon substrate prior to any functionalization. The refractive index of the subsequent layers was taken to be 1.5. Measurements from at least three regions of the sample were collected to obtain an average thickness. Measurements from three separate samples (*n* = 3) were averaged to obtain thickness values reported for each layer.

Design of a Microfluidic Device Used for Cell Capture. The microfluidic devices used for cell capture experiments were described in detail in our previous publication.¹⁷ Briefly, PDMS-based microfluidic devices with imbedded channel architecture were fabricated using standard soft lithography approaches.³⁸ Inlet/outlet holes were then punched with a blunt 16 gauge needle. Each microfluidic device contained two flow chambers with width-length-height dimensions of 3 × 10 × 0.1 mm and a network of independently addressed auxiliary channels (Figure 1B). The auxiliary channels were used to

apply negative pressure (vacuum suction) to the PDMS mold and secure it to the glass substrate. This strategy allows for the reversible sealing of a fluid conduit on top of aptamer-functionalized glass regions.

One milliliter syringes were connected by Tygon tubing (1/32 in. i.d., Fisher) to the outlets of each flow chamber with a metal insert cut from a 20 gauge needle. Blunt, shortened 20 gauge needles carrying plastic hubs were inserted into each inlet. A pressure-driven flow in the microdevice was created by withdrawing the syringe positioned at the outlet with a precision syringe pump (Harvard Apparatus, Boston, MA).

The two-channel microfluidic device was placed on top of the maleimide-functionalized substrate. Each chamber was filled with a specific concentration of thiolated anti-CD4 aptamer using a micropipet. Aptamers were immobilized on the surface through maleimide–thiol coupling (Figure 1B). The microfluidic device was then connected to a syringe pump as described above. After 2 h incubation with thiolated aptamer solution, chambers were flushed with 1x PBS–MgCl₂ and were ready for use in cell experiments. To serve as a positive control, certain channels were functionalized with antibodies against CD4 in lieu of anti-CD4 aptamer. In these cases, an identical procedure was followed with 1/5 μ M antibody solution replacing the aptamer solution.

Capturing Cells on Aptamer-Modified Surfaces. Molt-3 cells express CD4 antigen and therefore were chosen as model T-cells for aptamer cell capture experiments, whereas Daudi cells—a B-cell line—were used as CD4 negative controls. Flow cytometry was performed to confirm expression of CD4 on Molt-3 cells and lack of CD4 expression on Daudi cells. Both cell lines were cultured in suspension in 25 or 75 cm² tissue culture flasks at 37 °C in humidified atmosphere with 5% CO₂. Cells were incubated in RPMI-1640 supplemented with RPMI1640 medium containing 10% FBS and 1% penicillin/streptomycin. Since both Molt-3 and Daudi B cells are anchorage independent, they were collected from the tissue culture flask without trypsinization and concentrated by centrifugation prior to use.

Cells were then infused into microfluidic devices precoated with either aptamer or antibody-modified surfaces. In these experiments, surfaces were prepared using a range of CD4 aptamer concentrations (0, 1, 5, and 10 μ M) as well as two CD4 antibody concentrations (1 and 5 μ M). The solution of cell capture ligand was infused into one channel of the microfluidic device and incubated for 2 h to ensure immobilization. The other channel was functionalized with a linker and nonsense aptamer to serve as a negative control.

Subsequently, microfluidic devices were rinsed with 1x PBS and incubated with 1% (w/v) BSA for 1 h to passivate surfaces. After rinsing once again with binding buffer (1x PBS–MgCl₂), Molt-3 cells at a concentration of 10–20 million cells/mL were introduced into each channel at 10 μ L/min. Upon cell entry into each channel, flow was reduced to 1 μ L/min for 15 min to allow for cell attachment. This low flow rate was used to allow cells to interact with the aptamer-decorated surface. Afterward, channels were flushed thoroughly with PBS to remove nonspecifically adhered cells. Each channel was then incubated with 4% formalin solution for 15 min to fix captured cells prior to imaging. Bright-field images were taken with an Eclipse TS100 microscope equipped with phase contrast (Nikon, Inc.) at 10 \times magnification. Cell density was calculated by counting cells in at least three randomly selected regions in the middle of each channel. Errors reported represent one standard deviation.

Selective Capture of CD4 Expressing Cells from Cell Mixture. To better characterize specificity of cell capture, aptamer-functionalized surfaces were challenged with mixtures of CD4 (+) Molt-3 cells and CD4 (–) Daudi cells (Figure 1C). Molt-3 cells and Daudi B cells were stained green and red separately and then mixed at 15/85 and 25/75 proportions. 30 μ L of each mixture was loaded onto the inlet and flown through the aptamer-functionalized surface in the microfluidic device. Prior to cell seeding, the aptamer surface was rinsed with PBS–MgCl₂ binding buffer for 5 min. As mentioned in the preceding section, cells were introduced into the microfluidic device at the initial flow rate of 10 μ L/min. This flow rate was then lowered to 1 μ L/min to allow for cell attachment. After 15 min at this low flow rate,

unattached cells were washed away with 1x PBS under flow rate of 50 μ L/min. The cells captured on the surface were then imaged using a Zeiss LSM 5 Pascal confocal microscope (Carl Zeiss, Inc.).

RESULTS AND DISCUSSION

The objective of this paper was to characterize cell capture capacity of CD4 aptamer-modified surfaces. Our experiments demonstrate that aptamer-modified surfaces are as effective as antibodies in capturing CD4 expressing cells. These results may pave the way for future development of aptamer-containing devices for CD4 T-cell counting in HIV detection.

Construction and Characterization of Aptamer-Functionalized Surfaces. The silane modification scheme shown in Figure 1A led to incorporation of amine groups at the surface/solution interface. In the subsequent step, surfaces were functionalized using maleimide-PEG-NHS to introduce thiol reactive moieties. Finally, thiolated RNA aptamer specific to CD4 antigen was assembled on the surface. Every step in the construction of biointerface was verified by ellipsometry (Figure 2A).

Ellipsometry was also used to study aptamer–antigen interactions. In these experiments, some surfaces were modified

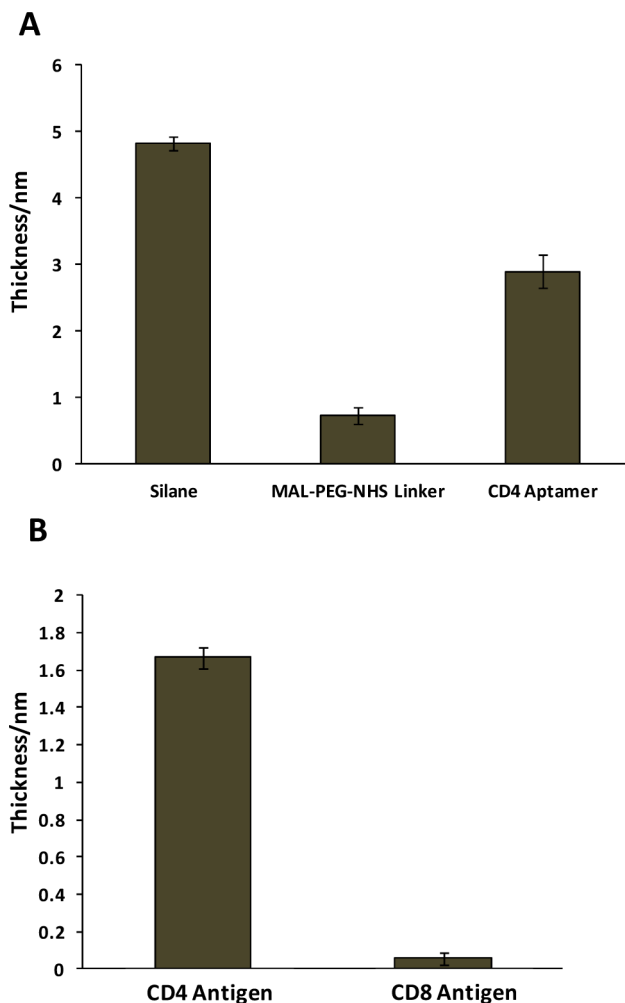


Figure 2. Ellipsometry characterization of bionterface layer assembly and aptamer–analyte interactions. (A) The change in thickness of molecular layers assembled on the surface. (B) The changes in thickness after aptamer-modified surfaces were challenged with CD4 protein (target analyte) and CD8 protein (nonspecific analyte).

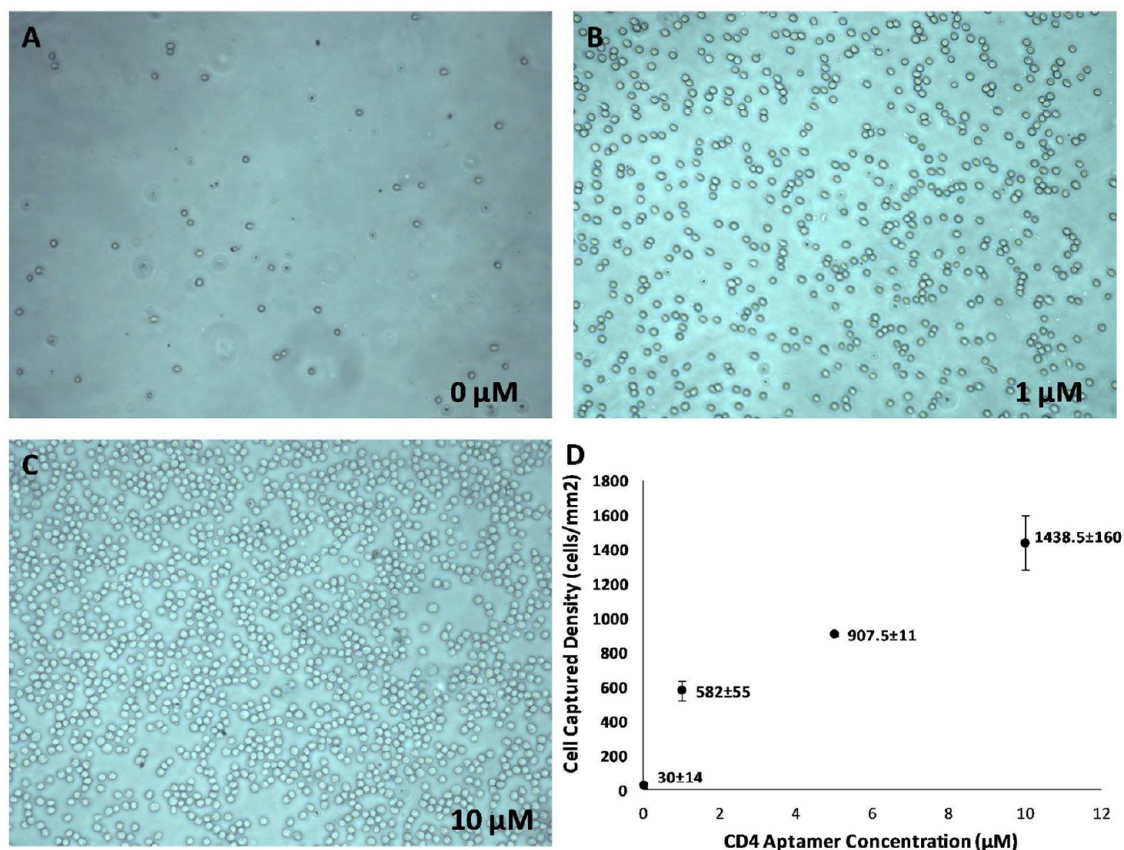


Figure 3. Cell capture density as a function of aptamer concentration. (A–C) Bright-field images of captured cells at 0, 1, and 10 μM . (D) The graph showing cell capture density as a function of aptamer concentration. Cell capture density varied from 582 ± 55 to 1438 ± 160 cells/ mm^2 with aptamer concentrations ranging 1 to 10 μM .

with CD4 aptamer while other substrates were functionalized with nonsense aptamer specific to IFN- γ .³⁵ These surfaces were challenged with recombinant CD4 protein as well as with CD8 antigen. As shown in Figure 2B, incubation with 10 μM CD4 antigen caused a thickness increase of 1.67 ± 0.59 nm, whereas incubation with the same concentration of CD8 resulted in minimal adsorption (0.06 ± 0.003 nm). No adsorption was observed after incubating nonspecific (IFN- γ) aptamer-functionalized surfaces with CD4 proteins (Figure S1).

Cell Capture on Aptamer-Modified Surfaces. CD4 expressing lymphocyte cell line Molt-3 was used to characterize cell capture on aptamer-functionalized surfaces. In the first set of experiments, the relationship between aptamer concentration and cell capture density was explored. The surfaces were prepared using aptamer solution concentrations ranging from 0 to 10 μM , integrated into microfluidic devices and challenged with the same concentration of Molt-3 cells (10 million/mL). The surfaces modified with either 1 or 5 μM antibody concentration served as positive controls while surfaces immobilized with nonsense aptamer used as negative controls in these experiments.

After channel functionalization, cells were seeded as described above. Capture density was determined by manual counting of cells in at least three bright-field fields of view from three separate devices. For each device, images were taken in the central region of the chamber to minimize the effects of nonspecific cell deposition around the inlets/outlets and channel edges. Results are shown in Figure 3. Cell capture density was observed to increase with aptamer concentration in

an approximate linear relationship (30 ± 14 , 582 ± 55 , 907 ± 11 , and 1438 ± 16 cells/ mm^2 for 0, 1, 5, and 10 μM aptamer, respectively (Figure 3)). For comparison, use of antibody-based capture surface under conditions found optimal in our previous experiments¹⁷ resulted in a capture density of 549 ± 13 and 815 ± 8 cells/ mm^2 for 1 and 5 μM concentrations.

The cell captured density under the same concentration for aptamer and antibody are compared in Figure 4. These data reveal that cell capture was similarly effective on aptamer- and antibody-functionalized surfaces. This is expected given that equilibrium constant (K_d) for the CD4 aptamer was reported to

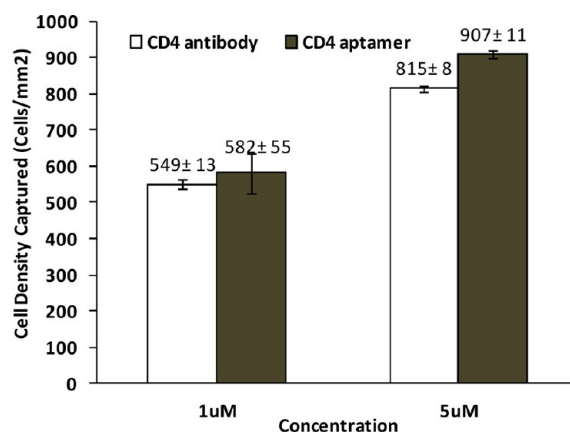


Figure 4. Comparison of Molt-3 cell density on surfaces modified with aptamer vs antibody molecules.

be 0.5 ± 0.07 nM,³⁴ while K_d for CD4 antibody (clone13B8.2) is 3.3 nM.³⁹ As a control experiment, Molt-3 cells were seeded onto surfaces functionalized with IFN- γ -aptamer serving as negative control. The density of cells on this nonspecific aptamer surface (39 ± 5 cells, see Figure S2A) was comparable to cell density on surfaces that did not contain aptamer at all (30 ± 14 cells/mm², see Figure 3A).

Selective Capture of CD4 Expressing Cells from a Heterogeneous Cell Suspension. To simulate an experiment where CD4 (+) cells will be present alongside CD4 (-) cells we created binary mixtures of CD4 expressing Molt-3 cells and Daudi cells. The latter cells come from B-cell lymphoma and do not express CD4. The cell types were labeled with green and red cell tracker dyes and then mixed at ratios of 15/85 and 25/75 of Molt-3 to Daudi cells. Given that CD4 cells represent ~10% of leukocytes in peripheral blood and 25–30% of mononuclear cells, the fractions used here mimicked the composition of physiologically relevant cell preparations. In a typical experiment, 30 μ L of cell suspension was loaded onto the inlet reservoir and infused into the microfluidic device for 15 min at 1 μ L/min. The chambers were then washed with 1x PBS at 50 μ L/min to remove unattached cells. Images in Figure 5A–D demonstrate selective sorting of CD4 expressing cells (labeled with green dye) on aptamer-functionalized surfaces. One should note that the volume of each microfluidic channel is ~ 3 μ L, whereas the volume of cell suspension infused and

pushed through the channel is 30 μ L. Because each channel is exposed to ~ 10 times the volume, the cells accumulate on the surface. This is why CD4 cell density at the start of cell capture experiment (Figure 5A,C) is much lower than the cell density after completion of the experiment (Figure 5 B,D). Quantification of cell capture purity presented in Figure 5D shows that $\sim 94\%$ of bound cells expressed CD4. Given that initial fraction of Molt-3 in solution was 15% and 25%, 4–6-fold enhancement in cell density could be achieved on the capture surface (Figure 5E).

Additional negative control experiments were carried out whereby only Daudi cells were incubated with aptamer-modified microfluidic devices using the same protocol as described for Molt-3/Daudi mixtures. In the case when these CD4 (-) cells interacted with CD4 aptamer-modified surfaces only minimal adhesion (25 ± 4 cells/mm², see Figure S2B) was observed, pointing once again to specificity of CD4 cell capture on aptamer surfaces.

CONCLUSION

The goal of the present paper was to fabricate and characterize aptamer-functionalized surfaces for capture of CD4 expressing cells. Surfaces containing RNA CD4 aptamer were first shown to be specific for binding CD4 proteins and were subsequently used for capture of CD4 expressing T-cells. Our experiments show that surfaces functionalized with aptamers are as effective as antibody-modified surfaces in capturing CD4 cells. Experiments aimed at challenging surfaces with mixtures of specific and nonspecific cells showed 6-fold enhancement in density of CD4 expressing cells on aptamer-modified substrates. Molt-3 cell purity of 94% was achieved from initial mixtures where Molt-3 cells represented only 15% and 25% of the cell population.

While labeling of CD4 T-cells with aptamers has been demonstrated,³⁴ to the best of our knowledge this is the first report of CD4 cell capture on aptamer-functionalized surfaces. Given enhanced thermal and chemical stability of aptamers and the importance of CD4 cell capture in HIV/AIDS monitoring, these surfaces may be applicable for future point of care blood analysis. In addition, the possibility of converting aptamers into reagentless biosensors may be leveraged in the future to create novel strategies for sensing CD4 cell binding.

ASSOCIATED CONTENT

Supporting Information

Figures S1 and S2. This material is available free of charge via the Internet at <http://pubs.acs.org>.

AUTHOR INFORMATION

Corresponding Author

*E-mail arevzin@ucdavis.edu; Ph 530-752-2383; Fax 530-754-5739.

Notes

The authors declare no competing financial interest.

ACKNOWLEDGMENTS

We thank Dr. Michael Howland for critical review of the paper. This work was supported by an NSF EFRI grant No. 0937997. J.S. was funded by fellowships from NIH (GM 56765 and ST32EB003827).

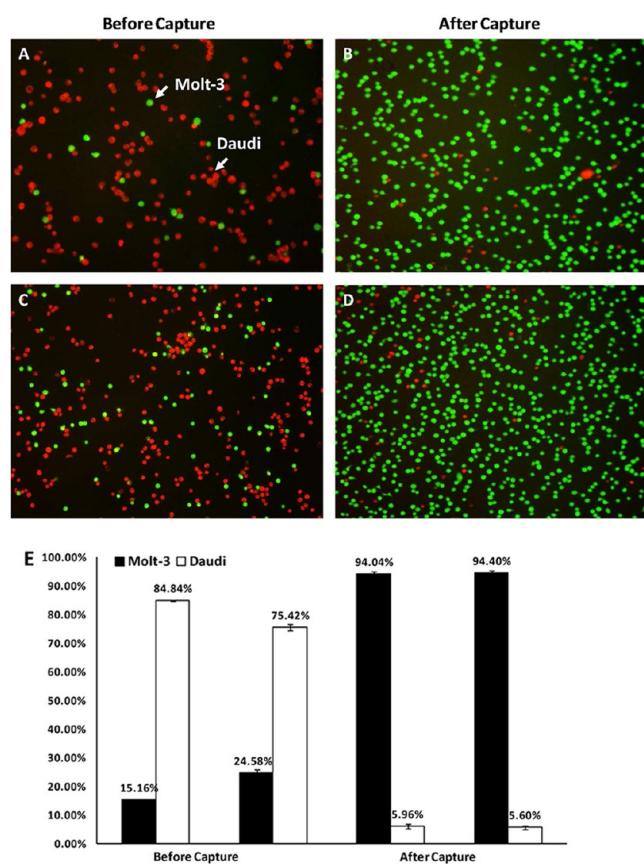


Figure 5. Capture of CD4 expressing cells from binary cell mixtures. (A–D) Images of cells. The experiments were performed in triplicate ($n = 3$ before and after cell capture). The Molt-3 cells (CD4+) were stained green while Daudi cells (CD4-) were stained red. (E) Quantifying Molt-3 and Daudi cell ratios before and after incubation with aptamer-functionalized surface.

REFERENCES

- (1) Salgame, P.; Abrams, J. S.; Clayberger, C.; Goldstein, H.; Convit, J.; Modlin, R. L.; Bloom, B. R. Differing lymphokine profiles of functional subsets of human CD4 and CD8 T cell clones. *Science* **1991**, *254* (5029), 279–82.
- (2) Sen, Y.; Chunsong, H.; Baojun, H.; Linjie, Z.; Qun, L.; San, J.; Qiuping, Z.; Junyan, L.; Zhang, X.; Jinqun, T. Aberration of CCR7 CD8 memory T cells from patients with systemic lupus erythematosus: an inducer of T helper type 2 bias of CD4 T cells. *Immunology* **2004**, *112* (2), 274–89.
- (3) Umetsu, D. T.; DeKruyff, R. H. TH1 and TH2 CD4+ cells in human allergic diseases. *J. Allergy Clin. Immunol.* **1997**, *100* (1), 1–6.
- (4) Umetsu, D. T.; DeKruyff, R. H. Th1 and Th2 CD4+ cells in the pathogenesis of allergic diseases. *Proc. Soc. Exp. Biol. Med.* **1997**, *215* (1), 11–20.
- (5) Gujar, S. A.; Jenkins, A. K.; Guy, C. S.; Wang, J.; Michalak, T. I. Aberrant lymphocyte activation precedes delayed virus-specific T-cell response after both primary infection and secondary exposure to hepatitis B virus in the woodchuck model of hepatitis B virus infection. *J. Virol.* **2008**, *82* (14), 6992–7008.
- (6) Siliciano, R. F.; Lawton, T.; Knall, C.; Karr, R. W.; Berman, P.; Gergory, T.; Reinherz, E. L. Analysis of host-virus interactions in AIDS with Anti-gp120 T cell clones: effect of HIV sequence variation and a mechanism for CD4+ cell depletion. *Cell* **1988**, *54*, 561–575.
- (7) Veazey, R. S.; DeMaria, M.; Chalifoux, L. V.; Shvets, D. E.; Pauley, D. R.; Knight, H. L.; Rosenzweig, M.; Johnson, R. P.; Desrosiers, R. C.; Lackner, A. A. Gastrointestinal tract as a major site of CD4+ T cell depletion and viral replication in SIV infection. *Science* **1998**, *280*, 427–431.
- (8) Veazey, R. S.; Marx, P. S.; Lackner, A. A. The mucosal immune system: primary target for HIV infection and AIDS. *Trends Immunol.* **2001**, *11*, 626–633.
- (9) Zenewicz, L. A.; Antov, A.; Flavell, R. A. CD4 T-cell differentiation and inflammatory bowel disease. *Trends Mol. Med.* **2009**, *15* (5), 199–207.
- (10) Toner, M.; Irimia, D. Blood-on-a-Chip. *Annu. Rev. Biomed. Eng.* **2005**, *7*, 77–103.
- (11) Revzin, A.; Maverakis, E.; Chang, H. C. Biosensors for immune cell analysis—A perspective. *Biomicrofluidics* **2012**, *6* (2), 021301–13.
- (12) Murthy, S. K.; Sin, A.; Tompkins, R. G.; Toner, M. Effect of flow and surface conditions on human lymphocyte isolation using microfluidic chambers. *Langmuir* **2004**, *20*, 11649–11655.
- (13) Sin, A.; Murthy, S. K.; Revzin, A.; Tompkins, R. G.; Toner, M. Enrichment using antibody-coated microfluidic chambers in shear flow: Model mixture of human lymphocytes. *Biotechnol. Bioeng.* **2005**, *91*, 816–826.
- (14) Sekine, K.; Revzin, A.; Tompkins, R. G.; Toner, M. Panning of multiple leukocyte subsets on antibody-decorated poly(ethylene) glycol-coated glass slides. *J. Immunol. Methods* **2006**, *313*, 96–109.
- (15) Cheng, X. H.; Irimia, D.; Dixon, M.; Sekine, K.; Demirci, U.; Zamir, L.; Tompkins, R. G.; Rodriguez, W.; Toner, M. A microfluidic device for practical label-free CD4+T cell counting of HIV-infected subjects. *Lab Chip* **2007**, *7* (2), 170–178.
- (16) Zhu, H.; Macal, M.; George, M. D.; Dandekar, S.; Revzin, A. A miniature cytometry platform for capture and characterization of T-lymphocytes from human blood. *Anal. Chim. Acta* **2008**, *608*, 186–196.
- (17) Zhu, H.; Stybayeva, G. S.; Macal, M.; George, M. D.; Dandekar, S.; Revzin, A. A Microdevice for multiplexed detection of T-cell secreted cytokines. *Lab Chip* **2008**, *8*, 2197–2205.
- (18) Cheng, X. H.; Gupta, A.; Chen, C. C.; Tompkins, R. G.; Rodriguez, W.; Toner, M. Enhancing the performance of a point-of-care CD4+T-cell counting microchip through monocyte depletion for HIV/AIDS diagnostics. *Lab Chip* **2009**, *9* (10), 1357–1364.
- (19) Stybayeva, G.; Mudanyali, O.; Seo, S.; Silangcruz, J.; Macal, M.; Ramanculov, E.; Dandekar, S.; Erlinger, A.; Ozcan, A.; Revzin, A. Lensfree holographic imaging of antibody microarrays for high-throughput detection of leukocyte numbers and function. *Anal. Chem.* **2010**, *82* (9), 3736–3744.
- (20) Cheng, X.; Liu, Y. S.; Irimia, D.; Demirci, U.; Yang, L. J.; Zamir, L.; Rodriguez, W. R.; Toner, M.; Bashir, R. Cell detection and counting through cell lysate impedance spectroscopy in microfluidic devices. *Lab Chip* **2007**, *7* (6), 746–755.
- (21) Watkins, N.; Venkatesan, B. M.; Toner, M.; Rodriguez, W.; Bashir, R. A robust electrical microcytometer with 3-dimensional hydrofocusing. *Lab Chip* **2009**, *9* (22), 3177–3184.
- (22) Ellington, A. D.; Szostak, J. W. In vitro selection of RNA molecules that bind specific ligands. *Nature* **1990**, *346* (6287), 818–822.
- (23) Hamaguichi, N.; Ellington, A. D.; Stanton, M. Aptamer beacons for the direct detection of proteins. *Anal. Biochem.* **2001**, *294*, 126–131.
- (24) Li, J. J.; Fang, X.; Tan, W. Molecular aptamer beacons for real-time protein recognition. *Biochem. Biophys. Res. Commun.* **2002**, *292*, 31–40.
- (25) Xiao, Y.; Lubin, A. A.; Heeger, A. J.; Plaxco, K. W. Label-free electronic detection of thrombin in blood serum by using an aptamer-based sensor. *Angew. Chem., Int. Ed.* **2005**, *44* (34), 5456–5459.
- (26) Xiao, Y.; Piorek, B. D.; Plaxco, K. W.; Heeger, A. J. A reagentless signal-on architecture for electronic, aptamer based sensors via target-induced strand displacement. *J. Am. Chem. Soc.* **2005**, *127*, 17990–17991.
- (27) Guo, K. T.; Schaffer, R.; Paul, A.; Gerber, A.; Ziemer, G.; Wendel, H. P. A new technique for the isolation and surface immobilization of mesenchymal stem cells from whole bone marrow using high-specific DNA aptamers. *Stem Cells* **2006**, *24* (10), 2220–31.
- (28) Pu, Y.; Zhu, Z.; Liu, H. X.; Zhang, J. N.; Liu, J.; Tan, W. H. Using aptamers to visualize and capture cancer cells. *Anal. Bioanal. Chem.* **2010**, *397* (8), 3225–3233.
- (29) Xu, Y.; Phillips, J. A.; Yan, J. L.; Li, Q. G.; Fan, Z. H.; Tan, W. H. Aptamer-based microfluidic device for enrichment, sorting, and detection of multiple cancer cells. *Anal. Chem.* **2009**, *81* (17), 7436–7442.
- (30) Phillips, J. A.; Xu, Y.; Xia, Z.; Fan, Z. H.; Tan, W. Enrichment of cancer cells using aptamers immobilized on a microfluidic channel. *Anal. Chem.* **2009**, *81* (3), 1033–9.
- (31) Dharmasiri, U.; Balamurugan, S.; Adams, A. A.; Okagbare, P. I.; Obubuafo, A.; Soper, S. A. Highly efficient capture and enumeration of low abundance prostate cancer cells using prostate-specific membrane antigen aptamers immobilized to a polymeric microfluidic device. *Electrophoresis* **2009**, *30* (18), 3289–300.
- (32) Martin, J. A.; Phillips, J. A.; Parekh, P.; Sefah, K.; Tan, W. Capturing cancer cells using aptamer-immobilized square capillary channels. *Mol. Biosyst.* **2011**, *7* (5), 1720–7.
- (33) Wan, Y.; Mahmood, M. A. I.; Li, N.; Allen, P. B.; Kim, Y.-t.; Bachoo, R.; Ellington, A. D.; Iqbal, S. M. Nanotextured substrates with immobilized aptamers for cancer cell isolation and cytology. *Cancer* **2012**, *118* (4), 1145–1154.
- (34) Davis, K. A.; Abrams, B.; Lin, Y.; Jayasena, S. D. Staining of cell surface human CD4 with 2'-F-pyrimidine-containing RNA aptamers for flow cytometry. *Nucleic Acids Res.* **1998**, *26* (17), 3915–3924.
- (35) Liu, Y.; Tuleouva, N.; Ramanculov, E.; Revzin, A. Aptamer-based electrochemical biosensor for interferon gamma detection. *Anal. Chem.* **2010**, *82* (19), 8131–8136.
- (36) Tuleuova, N.; Jones, C. N.; Yan, J.; Ramanculov, E.; Yokobayashi, Y.; Revzin, A. Development of an aptamer beacon for detection of interferon-gamma. *Anal. Chem.* **2010**, *82* (5), 1851–1857.
- (37) Tuleuova, N.; Revzin, A. Micropatterning of aptamer beacons to create cytokine-sensing surfaces. *Cell. Mol. Bioeng.* **2010**, *3* (4), 337–344.
- (38) Whitesides, G. M.; Ostuni, E.; Takayama, S.; Jiang, X.; Ingber, D. E. Soft lithography in biology and biochemistry. *Annu. Rev. Biomed. Eng.* **2001**, *3*, 335–373.
- (39) Bès, C.; Troadec, S.; Chentouf, M.; Breton, H.; Dominique Lajoix, A.; Heitz, F.; Gross, R.; Plückthun, A.; Chardès, T. PIN-bodies: A new class of antibody-like proteins with CD4 specificity derived from the protein inhibitor of neuronal nitric oxide synthase. *Biochem. Biophys. Res. Commun.* **2006**, *343* (1), 334–344.